NÖHÜ Müh. Bilim. Derg. / NOHU J. Eng. Sci., 2024; 13(4), 1517-1525

Niğde Ömer Halisdemir Üniversitesi Mühendislik Bilimleri Dergisi
Niğde Ömer Halisdemir University Journal of Engineering Sciences

Araştırma makalesi / Research article

www.dergipark.org.tr/tr/pub/ngumuh / www.dergipark.org.tr/en/pub/ngumuh

Numerical analysis of debris cloud formation in UHMWPE wavy plates during hypervelocity impact

Hiper hız darbesi sırasında UHMWPE dalgalı plakalarda enkaz bulutu oluşumunun nümerik analizi

Asım Önder[1, *]

[1] *Eskişehir Technical University, Department of Mechanical Engineering, 26555, Eskişehir, Türkiye*

Abstract

This paper presents and analyses the numerical results of hypervelocity impact against ultra-high molecular weight polyethylene (UHMWPE) plates with four different surface wave profiles. UHMWPE wavy plates (WP) are intended to be used in Whipple Shield bumper plate, which is of paramount importance for space vehicles against micro-meteorite and orbital debris (MMOD) impact protection. Numerical work was carried out as a hybrid combination of smoothed particle hydrodynamics (SPH) and finite element modelling (FEM). Circular plates were subjected to hypervelocity impact of a spherical aluminium projectile travelling at 3000 m/s. The outcomes of the simulations were analysed in terms of debris cloud generation, projectile fragmentation, and impact energy dissipation performance of wavy plates, and compared with a conventional flat counterpart. Results of this study indicate that surface wave profile has a clear positive influence in terms of hypervelocity impact protection performance.

Keywords: Hypervelocity impact, Wavy plates, UHMWPE, SPH, Whipple shield

Öz

Bu çalışma, dört farklı yüzey dalgası profiline sahip ultra yüksek moleküler ağırlıklı polietilen (UHMWPE) plakalara karşı hiper hız etkisinin sayısal sonuçlarını sunmakta ve analiz etmektedir. UHMWPE dalgalı plakaların (WP), mikro göktaşı ve yörünge enkazına (MMOD) karşı darbe korumasında, uzay araçları için büyük önem taşıyan Whipple Kalkanı tampon plakasında kullanılması amaçlanmaktadır. Nümerik çalışma, yumuşatılmış parçacık hidrodinamiği (SPH) ve sonlu elemanlar modellemesinin (FEM) hibrit bir kombinasyonu olarak gerçekleştirilmiştir. Dairesel plakalar, 3000 m/s hızla hareket eden küresel bir alüminyum merminin hiper hızda çarpma etkisine maruz bırakılmıştır. Simülasyon sonuçları dalgalı plakaların enkaz bulutu oluşumu, mermi parçalanması ve darbe enerjisi dağıtma performansı açısından analiz edilmiştir ve geleneksel düz bir muadiliyle karşılaştırılmıştır. Bu çalışmanın sonuçları, yüzey dalga profilinin hiper hız darbesinden korunma performansı açısından açık bir şekilde olumlu etkiye sahip olduğunu göstermektedir.

Anahtar kelimeler: Hiperhızlı darbe, Dalgalı plakalar, UHMWPE, SPH, Whipple kalkanı

1 Introduction

Naturally occurring (macro/micro meteorites) or man-made objects (failed structures during space missions) freely floating in space are a constant threat to existing space missions. This threat is generally termed as micro meteorite and orbital debris – MMOD. When these objects come in contact with space vehicles, the outcome can be catastrophic as they can have tremendous amount of impact energy due to their very high velocities (>2000 m/s). In 1947, Fred Whipple introduced the multi-layer shielding system for the protection of space vehicles [1]. It is called the Whipple shield and the concept has been studied for many years by many researchers in the field [2–6]. The shielding concept continues to bear research value due to the latest two reports from European Space Agency [7,8], stating that the number of the free-floating objects is ever increasing.

A Whipple shield consists of an outer plate called bumper plate, an inner plate called pressure wall/witness plate, and a gap between these two plates. Bumper plate's function is generally to disintegrate the incoming objects and disperse it as a debris cloud through the gap between the two layers in order to dissipate the impact energy.

To this date, Whipple shield configurations were investigated by researchers in the field from different perspectives. Christiansen and others studied the "stuffed" Whipple shield, introducing Nextel and Kevlar fabric in between aluminium bumper and rear wall plate [4]. Cour-Palais and Crews investigated multi-layer shock absorbing systems for NASA [9]. Nam and co-workers used aramid-epoxy composite material for their Whipple shiled [10]. Ke and co-workers also studied stuffed Whipple Shield, but differently than previous versions, they introduces polymer foam material to the configuration [11]. Baluch, Park and Kim investigated Whipple Shields made out of carbon-epoxy composite laminates under oblique hypervelocity impact conditions [12]. Rogers and co-workers studied the response of ultra-high molecular weight polyethylene (UHMWPE) and high density polyethylene (HDPE thermoplastics to hypervelocity impact on flat Whipple Shields [13]. Pai and

* Sorumlu yazar / Corresponding author, e-posta / e-mail: aaonder@eskisehir.edu.tr (A. Önder)
Geliş / Recieved: 21.08.2024 Kabul / Accepted: 27.09.2024 Yayımlanma / Published: 15.10.2024
doi: 10.28948/ngmuh.1536717

other studied the effect of coating on the bumper shield plates when subjected to hypervelocity impact [14].

Existing literature showed that every Whipple shield incorporated flat bumper plates regardless of the configurations investigated. To freshen the interest in the subject, a very recent effort has been made by the author of this paper, and wave profiles were introduced to bumper plates instead of flat surfaces. This study is a follow up to the author's recently published paper [15], and it contributes to the existing literature by extending the newly proposed wavy plate (WP) concept through the use of a completely different material (UHMWPE) compared to the previous research.

Four UHMWPE bumper plates with different surface wave profiles were studied under hypervelocity impact condition. Initial velocity of the aluminium spherical projectile was defined as 3000 m/s. WPs' behaviour on projectile fragmentation and debris cloud generation was investigated and compared both within each other and with flat bumper plate as well. In addition, performances of WPs to absorb and dissipate impact energy were presented.

2 Material and method

2.1 Materials and surface wave geometry

Since this paper extends the previous published study of the author [15], most of the details regarding the elements of the numerical modelling stay the same, except for the material used (hence material models) for WPs. Therefore, for the sake of conciseness, a brief description of those elements is provided here, however the parent study could be viewed for further specific details if needed.

Hypervelocity impact scenario studied in this paper consists of three elements: spherical impactor representing space debris; flat/wavy plate representing the bumper plate of a Whipple Shield; and finally witness plate representing the wall of a pressured space vessel.

Aluminium spherical projectile with a 5 mm diameter was used in all the simulations as the impacting object. Impact velocity was chosen as 3000 m/s for comparison with the previous studies and for staying inside the validated material model boundaries. Four different surface wave profiles (WP1 to WP4) were considered, and their geometric details can be seen in Figure 1 All the WPs have 1 mm of section thickness, and they are 50 mm in diameter. Design rationale of these WPs was to gradually deviate from flatness: i.e., WP4 has a shallower wave depth compared to others, while WP3 has a deeper wave depth, and so on. These WPs were compared with the conventional flat plate Whipple Shield bumper plate in terms of their behaviour on disintegrating the projectile and also their destruction patterns to generate a debris cloud. UHMWPE composite material (under Dyneema commercial name) was used for flat plate and four WPs in all the hypervelocity impact simulations performed in this study. UHMWPE material is produced by gel-spinning followed by hot drawing. Fibres formed after this process can be oriented unidirectionally and hot-pressed into desired direction and layers to form a layered fibre reinforced composite material. For the present study, configuration of these fibres was cross-ply or [0°/90°], hence fibres are positioned along *x* (0°) and *y* (90°) direction (in-plane), providing an orthotropic material.

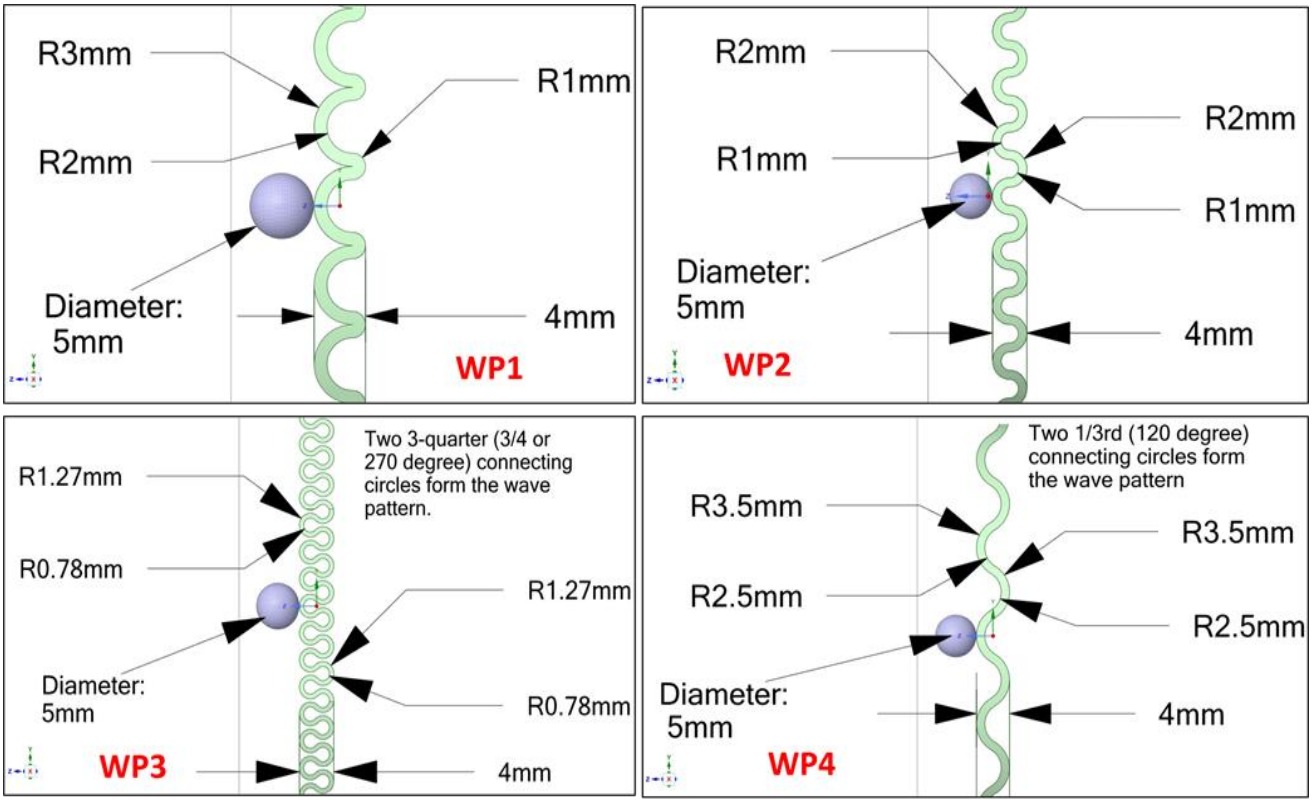

Figure 1. Section geometries of wave plates investigated in this study [15]

Al 1100 aluminium material was used for the spherical projectile. In order to assess the effect of debris cloud generated after impact, a witness plate is generally used behind the bumper plate. Al 2024-T4 aluminium material was considered for the witness plate which has 100x100x0.5 mm dimensions, which have been extensively used in the field by many researchers ([16–18]).

2.2 Numerical modelling

ANSYS Autodyn software was used for the hybrid numerical modelling performed in this study. Hybrid models incorporate the use of finite elements (FE) approach and smoothed particle hydrodynamics (SPH) approach together. SPH method is advantageous when extremely high loading and strain rates are of concern. These rates are so high that the solid material behaves almost like a fluid, even experiencing vaporisation due to the temperatures above melting temperature. In SPH method, material is represented by spherical particles with a certain size, and the movement of these particles allows the calculation of very large and quick deformations more effectively compared to FE approach. For this reason, SPH modelling is more suitable for the projectile and target bumper plate models as excessive deformation and failure behaviour happen during the hypervelocity impact phenomenon.

On the other hand, witness plate was modelled with finite element approach since the function of the witness plate in simulation is much less complex compared to the bumper plate, displaying only the extend and shape of failure.

Input data for the UHMWPE material model used in the simulations were obtained from Lassig and co-workers' extensive study [19]. As authors stated, this data set was validated with the physical testing carried out in the aforementioned reference (in Section 3.4 and Section 4 of [19]), in both quasi-static and dynamic environments. Input data of Al 1100 and Al 2024-T4 for the projectile and witness plate, respectively, was already present in the material library embedded in Autodyn software. Material data and modelling parameters regarding these materials can be found in Appendix at the end of this study.

Since very high strain rates are experienced during a hypervelocity impact, all three materials were modelled with a suitable shock equation of state material model. Linear Polynomial Equation of State (EOS) was used to model shock response of all the materials considered in this study. In addition to shock properties, Al 1100 and Al 024-T4 were modelled with Johnson-Cook Strength and Failure models, while UHMWPE material was modelled with Orthotropic Elasticity, and Orthotropic Failure and Softening material model. More details on theory can be found in [19] and [15] for UHMWPE and aluminium materials models, respectively.

The rest of the numerical model details are: 0.2 mm SPH particle size was used for both bumper plates and projectile, the witness plate was meshed using Lagrangian finite elements with a fixed 2 mm mesh size. Witness plate was modelled with zero degree of freedom from its four thin surfaces. For all impact scenarios, the projectile's impact trajectory direction was perpendicular.

3 Results and discussion

3.1 Analysis of fragmentation and debris cloud patterns

This section presents fragmentation of the projectile and the shape/characteristics of the debris cloud generated by the projectile and bumper plate after the hypervelocity impact. To ease the understanding, front, top, and right views of every plate were given. A general comparative figure (Figure 8) incorporating every plate investigated was also provided at the end of this section for a clear distinction. Firstly, the analysis of impact against flat plate is given to realise whether or not UHMWPE material influences the debris cloud characteristics compared to aluminium. Analysis of WPs will be presented next, revealing the differences and similarities compared to flat plate impact.

Figure 2 shows how the flat UHMWPE plate reacted to the impact. It can be clearly seen from front view that a cross shaped failure exists due to the fibre alignment along 0° (*x axis - horizontal*) and 90° (*y axis - vertical*). This is an indication that the shock wave created by the hypervelocity impact travels along fibre directions. This behaviour is different when compared to a metallic (isotropic material) plate counterpart, in which the shock wave travels in every direction, like an expanding circle in-plane (360° degree). When the shock wave reaches to the periphery of the plate, some part of it is reflected back from the plate boundary, and the remaining part causes tension loading to the fibres. This repetitive shock wave loading leads to fibre rupture which can be seen in Figure 2 along the fibre orientations. Shock waves travel in through-thickness direction as well and again they are partially reflected back and forth at the material boundary, which are the front and back side of the plate. Top and right views of Figure 2 show that same cross-shape failure along fibre directions existed at the back side of the plate as well.

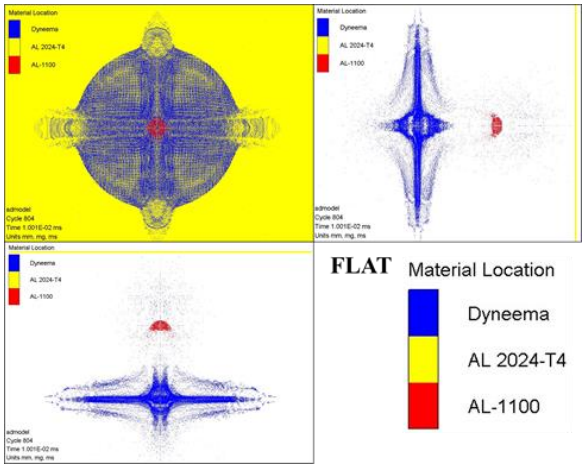

Figure 2. Front (top left), right (top right), and top (bottom left) views of the debris cloud in UHMWPE flat plate impact scenario at 10 µs

These observations are considerably different compared to an aluminium flat plate impact (Figure 3) which exhibits only a hole at the impact location slightly larger than the projectile diameter [15]. Debris cloud pattern and shape such as in Figure 3 formed from aluminium bumper material are reported by many researchers in literature, both experimentally and numerically [2,11,20–22].

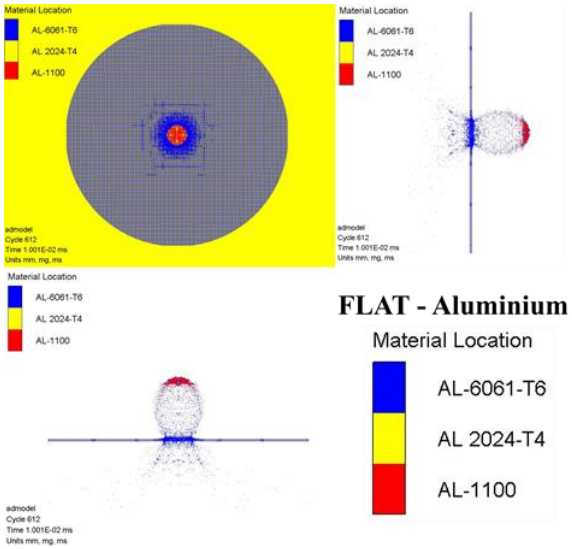

Figure 3. Front (top left), right (top right), and top (bottom left) views of the debris cloud in aluminium flat plate impact scenario at 10 µs

When UHMWPE flat plate and aluminium plate are compared (top and right views of Figure 2 and Figure 3), failure pattern influences the debris cloud generated after impact such that the horizontal and vertical spread angle of the plate particles at the impact location is greater and particles spread nonuniformly in UHMWPE impact case. These result in a less dense particle cloud generated at the vanguard of the projectile at the same time interval (10 µs).

On the other hand, fragmentation of the projectile in UHMWPE flat plate is similar to what has been observed in aluminium counterpart, but from Figure 2 and Figure 3, it can be said that aluminium plate is more effective in disintegrating the projectile, as greater portion of the projectile particles can be seen connected to each other in UHMWPE case.

Figure 4 through Figure 7 show the reaction of WPs to the hypervelocity impact with the same boundary and loading conditions mentioned earlier. One of the common observations for all the WPs is that the deformation in vertical direction caused by the impact failed to reach to the edges of each plate, unlike the deformation in horizontal direction, which separated WPs into two pieces. In addition, the failure and the resulting debris cloud occurred at the front surface (impact side) and the back surface are different for each respective WP. These outcomes are significantly different than what has been observed from both the aluminium flat plate impact reported in the existing literature, and from UHMWPE flat plate reported earlier in this study. This reaction can clearly be associated to the existence of wave patterns of each WP.

When the right and top views of each wave profile impact are compared in Figure 8, it can be seen that they resulted in a slightly different debris cloud at the back side of the WPs. The main reason for the debris cloud dispersion characteristic is the interaction timing and angle difference between the failed projectile particles and the shape of each wave pattern [15]. When the projectile deforms during the impact, failed particles at the front of the projectile starts to spread and move in vertical direction and meet with the bulges and dents of each wave pattern at a slightly different time and impact angle, generating a different debris cloud shape.

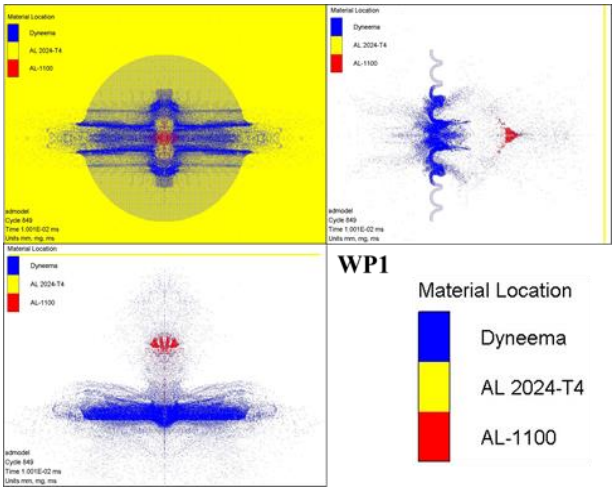

Figure 4. Front (top left), right (top right), and top (bottom left) views of the debris cloud in WP1 impact scenario at 10 µs

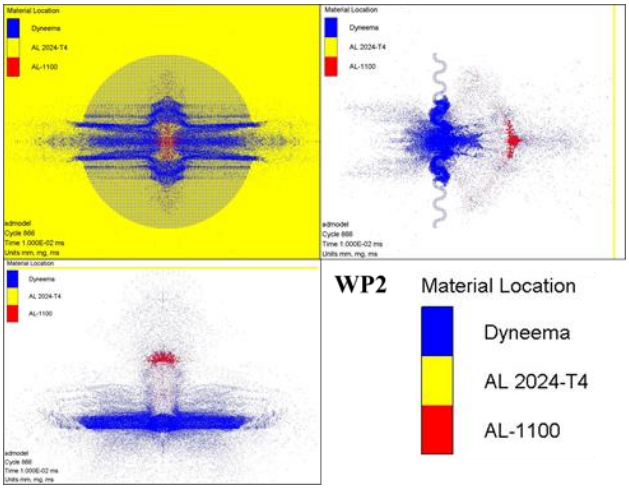

Figure 5. Front (top left), right (top right), and top (bottom left) views of the debris cloud in WP2 impact scenario at 10 µs

The largest spread of the debris cloud was observed for WP2, while in WP3 the debris cloud appeared as more confined compared to other WPs. WP1 exhibited similar debris cloud characteristics compared to WP2. WP4

experienced a vertically narrower debris cloud compared to the other WPs. In terms of projectile fragmentation, WP1, WP2, and WP4 causes a sharp-tipped deformation, while WP3 causes a blunt-tipped deformation compared to others as right views in Figure 8 show. Projectile particles were deformed more in vertical direction in WP2 compared to other WPs (Figure 5 and Figure 8). From the top views in Figure 8, it can be seen that all the projectiles were deformed similar to each other.

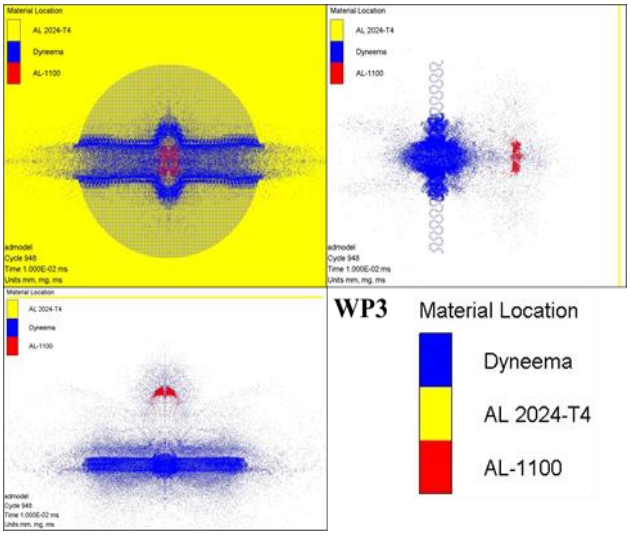

Figure 6. Front (top left), right (top right), and top (bottom left) views of the debris cloud in WP3 impact scenario at 10 µs

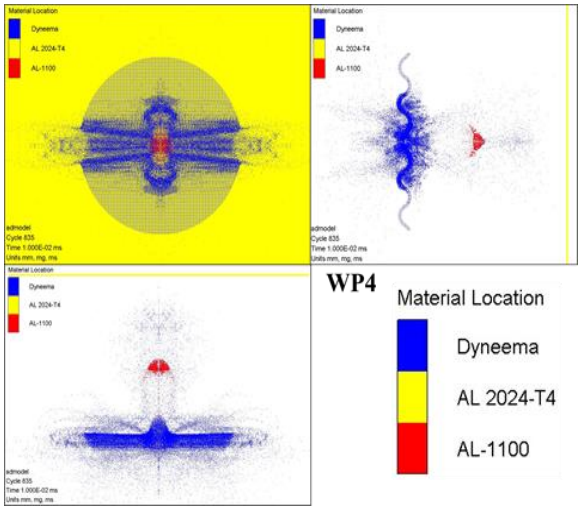

Figure 7. Front (top left), right (top right), and top (bottom left) views of the debris cloud in WP4 impact scenario at 10 µs

From the results given above, following discussions can be derived:

- Compared to flat plate counterpart, wave profile clearly has an influence on projectile fragmentation and debris cloud characteristics.
- WP4 has a shallower wave profile, while WP1, WP2, and WP3 has a deeper wave profile. Thus, deviation from flatness to waviness result in a more unorganised debris cloud as the impact of failed projectile fragments with the wave pattern becomes less predictable.
- On the other hand, as the wave pattern becomes deeper, the vanguard of the projectile becomes flatter during fragmentation. This is due to the fact that more material comes in contact with the projectile, hence providing more resistance.

In addition to the bumper plate failure analysis, an assessment of the potential hazard experienced from the debris cloud was also investigated by visual inspection of the damage done to the witness plate in every scenario. Thickness of each witness plate were deliberately selected as 2 mm to reveal the potential effect of the debris cloud. Since witness plate represents the outer most layer of a pressurised space vehicle, they are not designed as thin in a real-life case. Figure 9 shows the failure shape and dimensions of each witness plate positioned 50 mm away from the bumper plate. Obviously, as the distance between the bumper plate and witness plate changes, the distance that particles of the debris cloud travel changes as well, consequently affecting the characteristics of the damage done. However, there is no standard distance defined for a Whipple shield configuration and many different gaps were studied in the existing literature. For the sake of a lower computational effort and a faster calculation timing, distance between layers were selected as 50 mm.

From Figure 9, it can be seen that failure shapes and dimensions of each witness plate are similar. When compared with the flat counterpart, all WPs resulted in a debris cloud such that its effect on the witness plate deviates from a full circle to an ellipse shape. However, this effect is not straightforward as it was for the bumper plate. While witness plates of WP1 and WP2 has a narrower vertical failure compared to horizontal, witness plates of WP3 and WP4 has the opposite failure shape. Moreover, since WP4 has the shallowest wave profile and WP3 has the deepest wave profile, it is difficult to make a direct conclusion regarding the effect of wave profile on the witness plate failure shape.

It should be noted here that the main element of the debris cloud which causes complete perforation or rupture failure to the witness plate is the fragmented projectile. During the hypervelocity impact, the integrity of the projectile is greater compared to the bumper plate. Therefore, projectile is mainly responsible for the holes occurred in witness plate. On the other hand, particles of the bumper plate (mixed with projectile particles) are responsible for the secondary damage done to the witness plate. This secondary plastic failure can be seen at the inset of each WP in Figure 9. Bordered small green-red figures of each WP indicates the status of the Al 2024-T4 material. “Material Status” contour legend shows whether the material has voids (white), or it is in hydrostatic pressure (blue), elastic undamaged state (green), or in plastic failure state (red). Plastic failure (red areas) of each witness plate is considerably different than the other, and the difference is especially clear between the WPs and the flat plate.

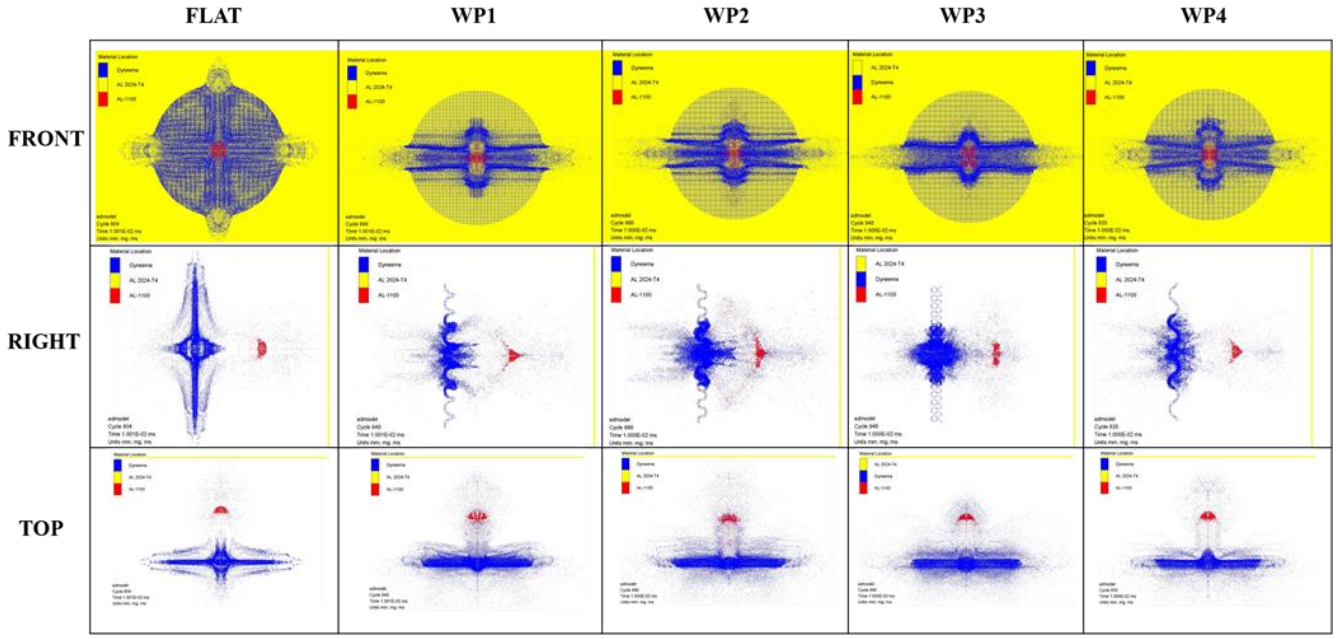

Figure 8. Overall comparison of front, right, and top views of WPs and flat plate at 10 µs

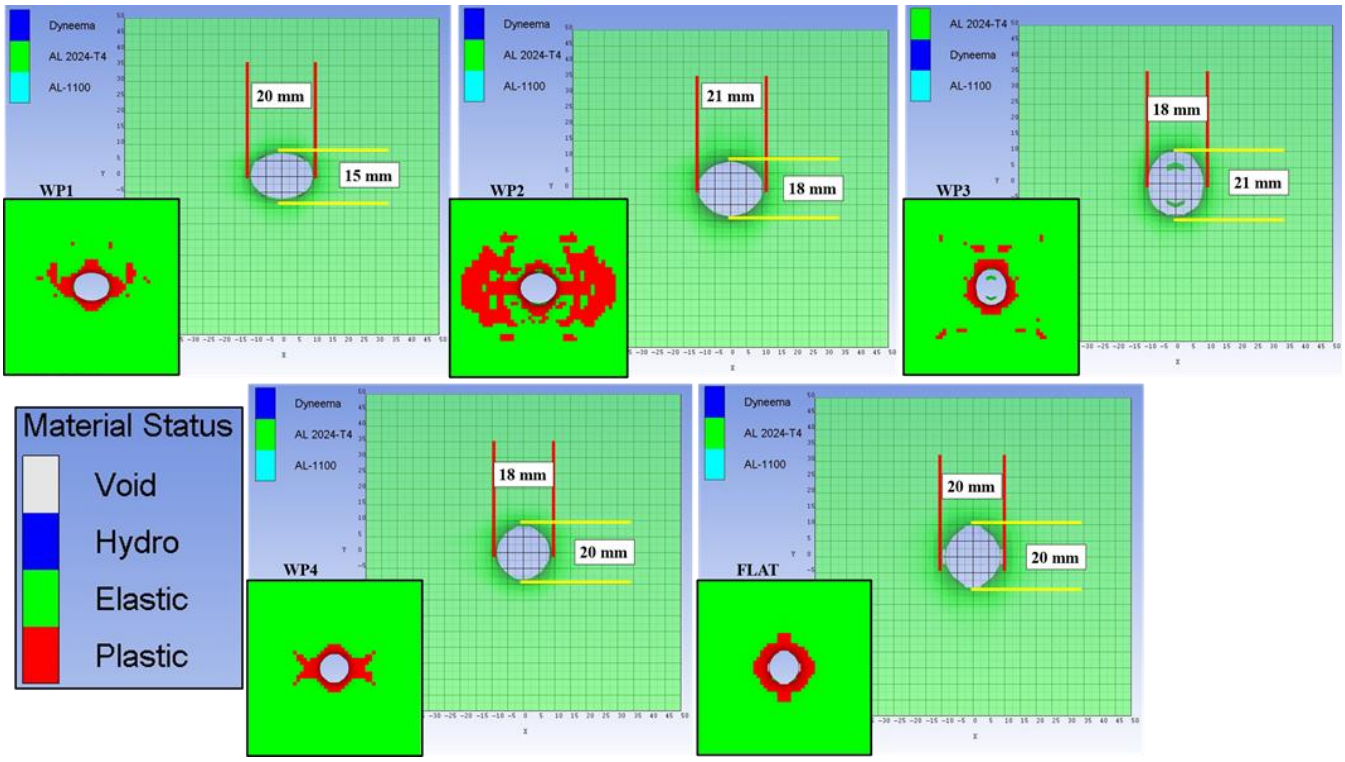

Figure 9. Comparison of witness plate (Al 2024-T4) damage in WPs and flat plate at the end of the simulations (at 50 µs)

In WP1, WP3, and WP4, plastic failure occurs in close perimeter of the hole, while in WP2 the plastic failure spread widely, almost reaching to the edges of the witness plate. This result makes the debris cloud generated by WP2 as the most hazardous compared to others. On the contrary, debris cloud generated by WP3 can be considered as the least hazardous since the areas exhibiting plastic failure are more scattered compared to WP1 and WP4 (even though the failure areas are similar).

3.2 Analysis of impact energy dissipation

Effectiveness of WPs was carried out through energy absorption analysis. During a hypervelocity impact, kinetic energy of the projectile is dissipated by various mechanisms such as failure of the bumper plate, mechanical contact

friction between bodies, and heat transfer mechanisms due to friction. In this study, the mass of the aluminium projectile was 0.18 gr. Combined with a 3000 m/s impact velocity, this mass results in an impact energy of 810 J. Figure 10 shows how the kinetic energy of the projectile changes during each hypervelocity impact against WPs and flat plate. There are two decreasing areas in the graph; the first one is right at the start of the impact which is due to the contact between the projectile and bumper plate, and the second one is when the fragmented projectile penetrates the bumper plate and comes into contact with the witness plate. Since witness plate represents the wall of a pressurised space vehicle and it is same for every scenario in this study, it is more important to evaluate the change in the kinetic energy before the projectile hits to the witness plate. As Figure 10 shows, every WP performed better than the flat plate, decreasing the kinetic energy of the projectile more compared to flat plate. WP2 appears as the most effective plate, followed by WP3 and WP1. WP4 displays the least performance among WPs, but still outperforms the flat plate. It can be derived from Figure 10 that a deeper wave pattern could be more effective in dissipating the impact energy.

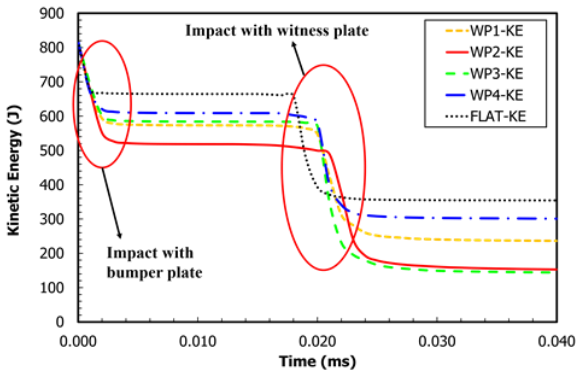

Figure 10. Kinetic energy change of the projectile during hypervelocity impact with WPs and flat plate

The decrease in projectile's kinetic energy indicates that a resistance is provided by the bumper plate, and this transferred impact energy causes deformation through various damage mechanisms. Therefore, bumper plate's internal energy increases as the projectile's kinetic energy decreases. Table 1 shows the change in internal energy of the WPs and flat plate at the end of the hypervelocity impact. In the same table, masses of each bumper plate were given as well to calculate the energy absorbed per mass (specific energy absorption) for a more meaningful comparison. In parallel with the kinetic energy dissipation, all the WPs outperformed flat plate in terms of energy absorption, WP3 and WP2 performing better compared to WP1 and WP4. From the specific energy absorption perspective, WP3 was ranked as first and WP1 was ranked as last, even lower than flat plate. This is an interesting finding since WP1 was the second best at decreasing the kinetic energy of the projectile and outperforming WP4 and flat plate.

Table 1. Impact energy absorbed by each plate

	Mass (gr)	Internal Energy (J)	Specific energy absorption (J/gr)
WP1	3.02	171	56.623
WP2	3.01	230	76.412
WP3	3.2	257	80.313
WP4	2.33	146	62.661
FP	1.92	125	65.104

3.3 General discussion

Previous sections analysed and explained the outcome of hypervelocity impact simulations and highlighted the important points and improvements. It is worth mentioning some details to avoid confusion and to reveal the potential of this study better.

The main aim of introducing a surface wave profile to the Whipple shield bumper plate is to enhance the protection ability of the shield configuration. This has been proven in a previously published study of the author [15] even though numerically. This study however was aimed to take the wave pattern concept a step further by investigating a completely different material. Previous study was done using an isotropic material (aluminium), but current study was carried out with an orthotropic/anisotropic material (UHMWPE fibre composite). This is a major difference because failure mechanisms of these two materials are completely different, composite material being much more complex. Therefore, results of this study also showed that a wave profile has a potential to be used with different material families.

It could be argued that the current study relies on only numerical results. It is true that a physical experimentation has not been done. However this does not mean the results are far from being practical, because the material model parameters used in this study were validated by respective authors (as cited previously) within the specific boundary conditions (velocity, temperature, pressure, etc.) used in this study. That is to say, if a material data was validated at e.g. 500 m/s impact condition, it is not reliable to use that data in e.g. 2000 m/s impact scenario, because the difference in velocities could well result in a considerable strain rate change, consequently the material behaviour could change as well. Nevertheless, this was not the case for the current study as the material model data is inside the validation conditions.

Another point that the reader might wonder is that the damage exhibited by the WPs investigated. In numerical study, the bumper plates could be seen ruptured horizontally. This is another major difference of UHMWPE compared to aluminium. However, this study focuses on the generation of the debris cloud which includes bumper plate and projectile particles, and its characteristics, because one of the main functions of the bumper plate is to disintegrate the incoming impacts from MMOD, turning them into a cloud of much smaller particles. So it can be considered as a sacrificial layer of the shielding system. Naturally, the integrity of the bumper plate is of course important, and it could be further investigated in a future study with bigger size plates. For the current study, in order to save computational effort, relatively smaller plates were considered. In addition, thickness of UHMWPE composite material in this study was 1 mm. Compared to an aluminium counterpart, this thickness

results in UHMWPE plate masses being approximately 1/3rd of the mass of the aluminium plates. So composite plates with higher thicknesses can be more beneficial and effective in future studies.

4 Conclusion

To extend the newly proposed wavy plate concept to a wider material family, this paper investigated the response of wavy bumper plates made out of UHMWPE against hypervelocity impact. What makes this study novel is the fact that no similar configuration (material-geometry) has been studied and reported before in the existing literature.

Four UHMWPE bumper plates with different surface wave profiles were subjected to hypervelocity impact of an aluminium spherical projectile travelling at 3000 m/s. Their behaviour on projectile fragmentation and debris cloud generation was investigated and compared both within each other and with flat bumper plate as well. In addition, performances of WPs to absorb and dissipate impact energy were presented.

Rupture of witness plates appear similar in each scenario with minor differences, but the plastic failure experienced by the witness plates were considerably different in WPs compared to flat plate. In addition, WPs have shown better performance in dissipating the kinetic energy of the projectile compared to the flat counterpart.

The results show that using orthotropic materials such as UHMWPE in Whipple Shield bumper plate with a wavy surface considerably changes the debris cloud characteristics and projectile fragmentation generated during a hypervelocity impact compared to a flat surface bumper plate. This can be considered as an improvement for the wavy bumper plate concept since previous research of wavy surface was incorporating isotropic materials such as aluminium. Therefore, it has been proven that additional family of materials have the potential to be used with a wavy surface in Whipple Shield configurations.

Conflict of interest

The author declares no conflict of interest.

Similarity rate (iThenticate): %19

References

[1] F.L. Whipple, Meteorites and space travel, Astronomical Journal, 52, 131, 1947. https://doi.org/10.1086/106009.

[2] M. V. Silnikov, I. V. Guk, A. F. Nechunaev, and N.N Smirnov, Numerical simulation of hypervelocity impact problem for spacecraft shielding elements, Acta Astronautica, 150, 56–62, 2018. https://doi.org/10.1016/j.actaastro.2017.08.030.

[3] S. Ryan and E. L. Christiansen, Hypervelocity impact testing of advanced materials and structures for micrometeoroid and orbital debris shielding, Acta Astronautica,83, 216–31, 2013. https://doi.org/10.1016/j.actaastro.2012.09.012.

[4] E. L. Christiansen, J. L. Crews, J. E. Williamsen, J. H. Robinson, and A. M. Nolen, Enhanced meteoroid and orbital debris shielding, International Journal of Impact Engineering, 17, 217–28, 1995. https://doi.org/10.1016/0734-743X(95)99848-L.

[5] A. Pai, R. Divakaran, S. Anand, and S. B. Shenoy, Advances in the Whipple Shield Design and Development: A Brief Review, Journal of Dynamic Behavior of Materials, 8, 20–38, 2022. https://doi.org/10.1007/s40870-021-00314-7.

[6] K. Wen, X. W. Chen, and Y. G. Lu, Research and development on hypervelocity impact protection using Whipple shield: An overview, Defence Technology, 17, 1864–86, 2021. https://doi.org/10.1016/j.dt.2020.11.005.

[7] S. Lemmens and F. Letizia, ESA'S Annual Space Environment Report, ESA Space Debris Office, Darmstadt, Germany, GEN-DB-LOG-00288-OPS-SD, 22 April 2022.

[8] S. Lemmens and F. Letizia, ESA's Annual Space Environment Report, Darmstadt, Germany, GEN-DB-LOG-00271-OPS-SD, 30 April 2019.

[9] B. G. Cour-Palais and J. L. Crews, A multi-shock concept for spacecraft shielding, International Journal of Impact Engineering, 10, 135–46, 1990. https://doi.org/10.1016/0734-743X(90)90054-Y.

[10] Y. W. Nam, S. K. Sathish Kumar, V. A. Ankem, and C. G. Kim, Multi-functional aramid/epoxy composite for stealth space hypervelocity impact shielding system, Composite Structures,193, 113–20, 2018. https://doi.org/10.1016/j.compstruct.2018.03.046.

[11] F. W. Ke, J. Huang, X. Z. Wen, Z. X. Ma, and S. Liu, Test study on the performance of shielding configuration with stuffed layer under hypervelocity impact, Acta Astronautica, 127, 553–60, 2016. https://doi.org/10.1016/j.actaastro.2016.06.037.

[12] A. H. Baluch, Y. Park, and C. G. Kim, Hypervelocity impact on carbon/epoxy composites in low Earth orbit environment, Composite Structures, 96, 554–60, 2013. https://doi.org/10.1016/j.compstruct.2012.09.010.

[13] J. A. Rogers, A. Mote, P. T. Mead, K. Harrison, G. D. Lukasik, K. R. Kota, W. D. Kulatilaka, J. W. Wilkerson, and T. E. Lacy, Hypervelocity impact response of monolithic UHMWPE and HDPE plates, International Journal of Impact Engineering, 161, 104081, 1-11, 2022. https://doi.org/10.1016/j.ijimpeng.2021.104081.

[14] A. Pai, A. Sharma, I. M. Eby, C. R. Kini, and S. B. Shenoy, A numerical approach for response of whipple shields with coated and monolithic front bumper to hypervelocity impact by spherical projectiles, Acta Astronautica, 202, 433–41, 2023. https://doi.org/10.1016/j.actaastro.2022.10.041.

[15] A. Önder, Projectile fragmentation and debris cloud formation behaviour of wavy plates in hypervelocity impact, International Journal of Impact Engineering, 183, 104788, 1-13, 2024. https://doi.org/10.1016/j.ijimpeng.2023.104788.

[16] Z. Song, X. Pei, J. Yu, J. Zhao, and F. Tan, Hypervelocity impact tests on a Whipple shield using a flyer plate in the velocity range from 4 km/s to 12 km/s, International Journal of Impact Engineering, 156,

103899, 1-14, 2021. https://doi.org/10.1016/j.ijimpeng.2021.103899.

[17] G. R. Johnson and W. H. Cook, A Computational Constitutive Model and Data for Metals Subjected to Large Strain, High Strain Rates and High Pressures, The Seventh International Symposium on Ballistics, pp. 541–547, Hague, Netherlands, 1983.

[18] H. B. Zeng, S. Pattofatto, H. Zhao, Y. Girard, and V. Fascio, Perforation of sandwich plates with graded hollow sphere cores under impact loading, International Journal of Impact Engineering, 37, 1083–91, 2010. https://doi.org/10.1016/j.ijimpeng.2010.05.002.

[19] T. Lässig, L. Nguyen, M. May, W. Riedel, U. Heisserer, H. Van Der Werff, and S. Hiermaier, A non-linear orthotropic hydrocode model for ultra-high molecular weight polyethylene in impact simulations, International Journal of Impact Engineering, 75, 110–22, 2015. https://doi.org/10.1016/j.ijimpeng.2014.07.004.

[20] K. Wen, X. W. Chen, R. Q. Chi, and Y. G. Lu, Analysis on the fragmentation pattern of sphere hypervelocity impacting on thin plate. International Journal of Impact Engineering, 146, 103721, 1-15, 2020. https://doi.org/10.1016/j.ijimpeng.2020.103721.

[21] K. Loft, M. C. Price, M. J. Cole, and M. Burchell, Impacts into metals targets at velocities greater than 1 km/s: A new online resource for the hypervelocity impact community and an illustration of the geometric change of debris cloud impact patterns with impact velocity, International Journal of Impact Engineering, 56, 47–60, 2013. https://doi.org/http://dx.doi.org/10.1016/j.ijimpeng.2012.07.007.

[22] J. Mespoulet, P. L. Héreil, H. Abdulhamid, P. Deconinck, and C. Puillet, Experimental study of hypervelocity impacts on space shields above 8 km/s, Procedia Engineering, 204, 508-515, 2017. https://doi.org/10.1016/j.proeng.2017.09.748.

Appendix

Numerical model parameters of Al 1100 and Al 2024-T4

Parameter (unit)	Al 1100	Parameter (unit)	Al 2024-T4
Johnson-Cook Strength		**Steinberg Guinan Strength**	
Shear Modulus (kPa)	2.59E+07	**Initial Yield Stress (kPa)**	2.60E+05
Yield Stress (kPa)	4.10E+04	**Max Yield Stress (kPa)**	7.60E+05
Hardening constant (kPa)	1.25E+05	**Hardening Constant**	310
Hardening exponent (none)	0.183	**Hardening Exponent**	0.185
Strain rate constant (none)	0.001	**Derivative dG/dP G'P**	1.8647
Thermal Softening Exponent (none)	0.859	**Derivative dG/dT G'T (Pa/C)**	-1.76E+07
Melting temperature (K)	893	**Derivative dY/dP Y'P**	0.01695
Reference Strain Rate (1/s)	1	**Melting Temperature (C)**	946.85
Johnson-Cook Failure		**Grady Spall Failure**	
Damage constant – D1(none)	0.071	**Critical Strain Value**	0.15
Damage constant – D2 (none)	1.248	**Shear Modulus (kPa)**	2.86E+07
Damage constant – D3 (none)	-1.142	**Shock EOS Linear**	
Damage constant – D4 (none)	0.0097	**Gruneisen Coefficient**	2
Damage constant – D5 (none)	0	**Parameter C1 (m/s)**	5328
Melting Temperature (K)	893	**Parameter S1**	1.338
Reference Strain Rate (1/s)	1	**Parameter Quadratic S2 (s/m)**	0
Linear Polynomial EOS			
Bulk Modulus – A1 (kPa)	7.42E+07		
Parameter A2 (kPa)	6.05E+07		
Parameter A3 (kPa)	3.65E+07		
Parameter B0 (none)	1.96		
Parameter B1 (none)	0		
Parameter T1 (kPa)	7.42E+07		
Parameter T2 (kPa)	0		
Reference Temperature (K)	293		
Specific heat (J/kgK)	910	**Specific Heat (J/kgK)**	863
Thermal conductivity (J/mKs)	0		

Numerical model parameters of UHMWPE (Dyneema)

Orthotropic linear elastic model (stiffnesses and Poisson's ratios)		Polynomial EOS (coefficients)		Orthotropic failure and softening (tens. fail. stresses and fracture toughnesses)	
E11 & E22 [GPa]	26.9	**A1 [GPa]**	7.04	**σ11fail & σ22fail [MPa]**	753
E33 [GPa]	3.62	**A2 [GPa]**	10	**σ33fail [MPa]**	1.07
ν12 [-]	0	**A3 [GPa]**	0	**τ31fail [MPa]**	1.01E+20
ν13 [-]	0.1	**B0 [-]**	3.864	**τ12fail [MPa]**	35.2
ν23 [-]	0.5	**B1 [-]**	3.864	**τ23fail [MPa]**	1.01E+20
G12 [MPa]	42.3	**T1 [GPa]**	7.04	**GC11 & GC22 [J/m2]**	30
G31 [MPa]	30.7	**T2 [GPa]**	0	**GC33 [J/m2]**	790
G23 [MPa]	30.7	**Tref [K]**	293	**GC31 [J/m2]**	1.46
		Spec. Heat [J/kgK]	1.85E+03	**GC12 [J/m2]**	1.46
		Thermal Conductivity	0	**GC23 [J/m2]**	1.46
				Dam. Coupl. Coeff.	5.00E-01

Orthotropic hardening model (coefficients and effective s-ε-values)					
Plasticity coefficients				**Effective stress-strain-values**	
a11 [-]	1.00E-05	**σeff#1 [kPa]**	1.76E+02	**εeff#1 [-]**	1.82E-04
a22 [-]	1.00E-05	**σeff#2 [kPa]**	9.89E+02	**εeff#2 [-]**	1.20E-03
a33 [-]	0.03	**σeff#3 [kPa]**	1.74E+03	**εeff#3 [-]**	3.11E-03
a12 [-]	1.00E-06	**σeff#4 [kPa]**	2.42E+03	**εeff#4 [-]**	6.92E-03
a13 [-]	1.00E-06	**σeff#5 [kPa]**	3.10E+03	**εeff#5 [-]**	1.13E-02
a23 [-]	1.00E-06	**σeff#6 [kPa]**	5.97E+03	**εeff#6 [-]**	2.83E-02
a44 [-]	1.75	**σeff#7 [kPa]**	1.20E+04	**εeff#7 [-]**	5.78E-02
a55 [-]	1.75	**σeff#8 [kPa]**	2.07E+04	**εeff#8 [-]**	1.06E-01
a66 [-]	1	**σeff#9 [kPa]**	3.46E+04	**εeff#9 [-]**	1.06E-01
		σeff#10 [kPa]	2.02E+08	**εeff#10 [-]**	1
Reference density [g/cm3]	9.80E-01				